Analysis of the interfaces of $[NiFe/Mo]_{30}$ and $[Fe/Mo]_{30}$ multilayers

1999 J. Phys.: Condens. Matter 11 945

(http://iopscience.iop.org/0953-8984/11/4/002)

J. Phys.: Condens. Matter **11** (1999) 945–954. Printed in the UK PII: S0953-8984(99)97254-5

Analysis of the interfaces of $[NiFe/Mo]_{30}$ and $[Fe/Mo]_{30}$ multilayers

G M Luo†, H W Jiang†, F Wu†, M L Yan†, Z H Mai†, W Y Lai†, C Dong† and Y T Wang‡

† Institute of Physics, and Centre of Condensed Matter Physics, Chinese Academy of Sciences, PO Box 603, Beijing 100080, People's Republic of China
‡ Institute of Semiconductors, Chinese Academy of Sciences, Beijing 100083, People's Republic of China

Received 1 September 1998, in final form 29 October 1998

Abstract. The interface states of $[NiFe/Mo]_{30}$ and $[Fe/Mo]_{30}$ multilayers have been investigated by x-ray small angle reflection and diffuse scattering. Significant interface roughness correlation was observed in both ultrathin $[NiFe/Mo]_{30}$ and $[Fe/Mo]_{30}$ multilayers. An uncorrelated roughness of about 2.7–3.1 Å was revealed in the $[NiFe/Mo]_{30}$ multilayers, which is explained as originating from a transition layer between the NiFe and the Mo layers. By the technique of diffuse scattering, it is clearly indicated that the interfacial roughness of NiFe/Mo is much smaller than that of Fe/Mo although the lattice mismatch is the same in both multilayers.

1. Introduction

The interfacial state is a major subject for the study of the giant magnetoresistance (GMR) effect of ultra-thin metallic multilayers [1]. It is widely accepted that the spin dependent electronic scattering at the interface plays an important role in defining the GMR effect. Previous studies on the role of the interface roughness on the GMR have been conducted by several authors [2, 3]. The rms of the interfacial roughness consists of both geometrical and intermixing parts [4, 5], but they will have different contributions to the GMR. It is important to draw a clear distinction between them. Such a detailed study of the interface could be helpful in understanding the magnetic properties of the multilayers. As is well known, the geometrical component of the roughness at the surface or interface induces diffuse scattering because it makes the Fourier spectrum of the electron density along the in-plane direction, q_x, non-zero in reciprocal space. The chemical intermixing at the interface produces no diffuse scattering because the intermixing only induces electron density changes in the normal direction, q_z. It is therefore possible to unambiguously separate the geometrical and intermixing components of the total interface width by analysing the transverse diffuse scatter.

In our previous work [6, 7], we reported that oscillations of the magnetic interlayer coupling were observed in NiFe/Mo multilayers, but that no GMR effect was observed. However, we did find evidence for both the oscillation of the magnetic interlayer coupling and the GMR effect in Fe/Mo multilayers. It was also found that a transition layer between the NiFe and Mo layers was present in the NiFe/Mo multilayers, while there was no such layer in the Fe/Mo multilayers.

0953-8984/99/040945+10$19.50

In this paper, we report the interfacial states of ultra-thin NiFe/Mo and Fe/Mo multilayers investigated by the techniques of x-ray small angle reflection and diffuse scattering. Different interfacial states were observed in these two multilayers, which is helpful in understanding their differing magnetic properties.

2. Theoretical background

As is well known, the x-ray small angle reflection theory and the x-ray diffuse scattering theory for multilayers were developed by Parrat [8], Sinha *et al* [9] and Holy *et al* [10, 11]. The recurrence method [8] is considered to be an effective method for the small angle reflection when the incident angle θ is larger than the critical angle of total reflectivity (θ_c). However. the distorted-wave Born approximation (DWBA) [9–11] should be used when the incident or transmitted angle is smaller than the critical angle θ_c for the transverse scan. In this paper, the recurrent method was used to simulate the small angle reflection curve, and the DWBA method was applied to the simulation of the transverse diffuse scatter.

To simulate the transverse scans, the correlation function of the ith and jth interfacial roughness is that introduced by Sinha *et al* [9], namely,

$$C_{i,j}(R) = \sigma_{cor}^2 \exp[-(R/\xi)^{2h}] \tag{1}$$

where $R = \sqrt{(x-x')^2 + (y-y')^2}$, (x, y) and (x', y') are the in-plane co-ordinates on the ith and jth interfaces respectively, σ_{cor} is the rms of the correlated roughness, ξ, the lateral correlation length and $D = 3 - h$ the fractal dimension.

The correlated roughness can be obtained from the ratio of the intensities of the diffuse scattering and specular reflectivity around the Bragg peak. The intensity of the specular reflectivity can be expressed as [4]:

$$I_{spec} = I_0 \exp(-q_z^2\sigma^2) \tag{2}$$

where $\sigma^2 = \sigma_{cor}^2 + \sigma_p^2$, where σ_p is the rms of the uncorrelated geometrical roughness, and the component of the roughness due to intermixing at the interface, q_z is the reflection vector normal to the surface and I_0 the total intensity. The diffuse scattering from the correlated roughness at different interfaces within the multilayer interferes with each other, and this interference confines the diffuse scatter to a region around the Bragg peak [4, 11]. When the transverse diffuse scan is performed with q_z at the Bragg peak, the integrated intensity of the diffuse scatter can be expressed as [4]:

$$I_{diff} = I_0 \exp(-q_z^2\sigma_p^2)[1 - \exp(-q_z^2\sigma_{cor}^2)]. \tag{3}$$

Thus we can obtain the correlated component, σ_{cor}, from the ratio of I_{diff}/I_{spec}.

3. Experiment

Both $[NiFe/Mo]_{30}$ and $[Fe/Mo]_{30}$ multilayers were deposited on water-cooled glass substrates by magnetron sputtering [6, 7]. $[NiFe/Mo]_{30}$ multilayers were grown with the thickness of the NiFe layer fixed to 17 Å and the thickness of the Mo layer was varied across a series of samples. In the $[Fe/Mo]_{30}$ multilayers, the thickness of the Fe layer was fixed to 12 Å, the thickness of the Mo layer varied. X-ray experiments were performed on a Rigaku diffractometer with a 12 kW rotating anode x-ray generator using a Cu target with a Ge(224) monochromator and a 0.2 mm narrow slit before the sample and the detector respectively. The divergent angle of the incident beam is 12 arc seconds and the entrance aperture angle, Ω_{ap}, of the detector is about 0.10°.

A specular reflectivity (θ–2θ) scan was performed in order to investigate the thickness of the films and to measure the total interfacial roughness. Longitudinal diffuse scans (θ–2θ offset scan) were carried out to confirm the existence of correlations of the interfacial roughness within the multilayers. The longitudinal scans are performed with the sample angle, θ, offset enough to avoid the specular peak. In order to measure the correlated component of the roughness, transverse scans were performed with the detector angle, 2θ, corresponding to the first Bragg peak.

4. Results and discussion

Figure 1 shows the small angle reflection (θ–2θ scan) and the longitudinal scan (θ–2θ offset scan) profile for an [NiFe/Mo]$_{30}$ multilayer, sample N1. The longitudinal scan was performed with θ offset by -0.13° to avoid the specular peak. From figure 1, it is clear that there is a strong enhancement of the diffuse scatter at the Bragg peak in the longitudinal scan, indicating that there is significant roughness correlation between the different interfaces within the multilayer. By simulating the small angle reflection curve, the thickness of NiFe and Mo layers was found to be 17.0 and 8.2 Å respectively (shown in table 1), and the rms of total interfacial roughness was $\sigma = 4.5 \pm 0.2$ Å.

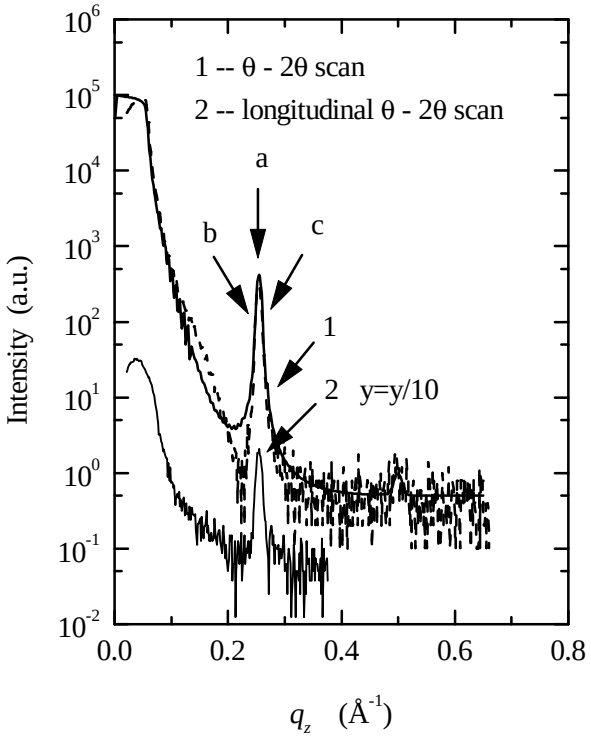

Figure 1. The small angle reflection and θ–2θ offset scan with θ offset -0.13° of [NiFe/Mo]$_{30}$ multilayers N1: dashed curves: 1—the small angle reflection curve, 2—the θ–2θ offset scan curve, solid curves: the simulated small angle reflection curve.

Table 1. The roughness of $[NiFe/Mo]_{30}$ multilayers obtained from the small angle reflection.

Sample	t_{NiFe} (Å)	t_{Mo} (Å)	σ (Å)
N1	17.0	8.2	4.5 ± 0.2
N2	17.0	16.5	5.0 ± 0.2
N3	20.5	13.5	3.0 ± 0.2

Table 2. Interface parameters σ_{cor}, ξ, h and σ_p of $[NiFe/Mo]_{30}$ multilayers obtained from the transverse diffuse scatter.

Sample	σ_{cor} (Å)	ξ (Å)	h	σ_p (Å)
N1	3.8 ± 0.2	<100	1.0 ± 0.1	2.7 ± 0.4
N2	3.9 ± 0.2	300 ± 50	1.0 ± 0.1	3.1 ± 0.4
N3	1.2 ± 0.2	500 ± 50	1.0 ± 0.1	2.7 ± 0.4

Figure 2 shows the transverse scans of sample N1. Profiles (*a*), (*b*) and (*c*) were measured with the detector angle fixed at the positions $2\theta = 3.58^\circ$ ($q_z = 0.255$ Å^{-1}), $2\theta = 3.50^\circ$ ($q_z = 0.250$ Å^{-1}) and $2\theta = 3.66^\circ$ ($q_z = 0.260$ Å^{-1}) respectively, as indicated in figure 1. One can see that all the curves are asymmetric because the illuminated area of the sample is proportional to $1/\sin\theta_1$, where θ_1 is the incident angle. The asymmetry also comes from the entrance aperture angle of the detector Ω_{ap}. The intensity as measured by the detector is expressed by [10]

$$I_{detector}(\theta_1, \theta_2) = I_{inc} \int_{\Omega_{ap}} \left(\frac{\mathrm{d}\sigma}{\mathrm{d}\Omega}\right)_{diff} \mathrm{d}\Omega. \tag{4}$$

The scattering vectors are given by

$$q_x = (2\pi/\lambda)(\cos\theta_1 - \cos\theta_2) \qquad q_z = (2\pi/\lambda)(\sin\theta_1 + \sin\theta_2) \tag{5}$$

where θ_2 is the transmitted angle, and λ the x-ray wavelength. Figure 3 shows the distribution of diffuse scattering intensity around the Bragg peak calculated using the DWBA approximation [10]. From figure 3 one can see that the x-ray refraction in the multilayer distorts the stripe of the diffuse scattering around the Bragg peak [10]. During the transverse diffuse scan the detector gathers the diffuse scattering intensity from different 2θ angles defined by an acceptance angle, $2\theta \pm \Omega_{ap}/2$, and furthermore, the intensity from different q_x and q_z. It is obvious that the entrance aperture angle of the detector Ω_{ap} can influence the asymmetry of the transverse scan.

From figure 2 one can see that the profiles (*a*), (*b*) and (*c*) display different shapes. This means that the x-ray refraction in the multilayer must be taken into account [10]. It is also apparent in figure 2 that there are no Yoneda peaks in any of the profiles, again indicating that a significant proportion of the roughness is correlated from the different interfaces throughout the multilayer.

The correlated roughness was calculated using the method described above and was found to be $\sigma_{cor} = 3.8 \pm 0.2$ Å. Simulations of the transverse scans obtained from sample N1, shown in figure 2, enable the lateral correlation length and fractal parameter to be calculated: $\xi < 100$ Å, $h = 1.0$. These parameters, listed in table 2, indicate that the interfaces of the $[NiFe/Mo]_{30}$ multilayer have a Gaussian nature [10]. Due to the restricted range of q_x that can be explored, we cannot obtain the value of ξ accurately when the lateral correlation length is less than 100 Å. By subtracting the correlated roughness from the total interface roughness (as deduced from the reflectivity simulations), the rms of the uncorrelated and intermixing component is deduced, in this case $\sigma_p = 2.7 \pm 0.6$ Å.

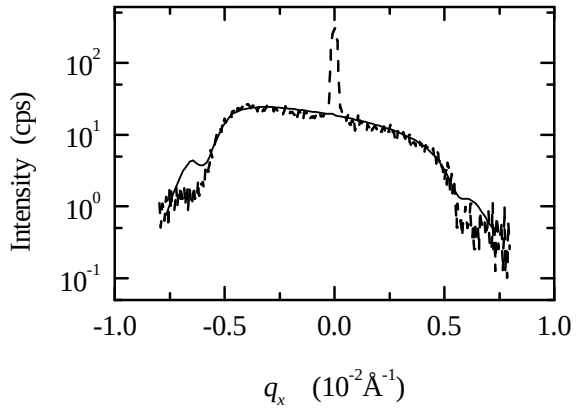

(*a*)

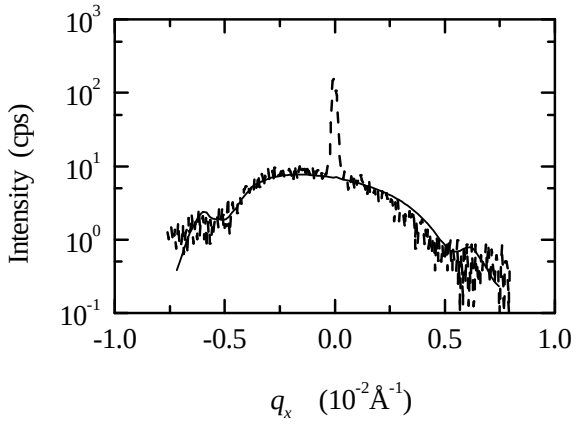

(*b*)

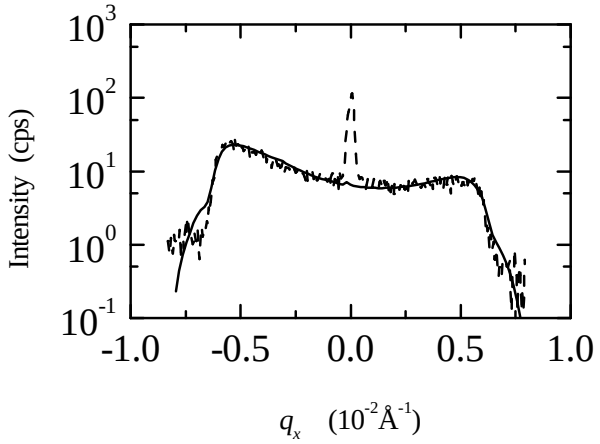

(*c*)

Figure 2. The transverse scan of sample N1: (*a*) peak position at $2\theta = 3.58^\circ$, $q_z = 0.255$ Å^{-1}; (*b*) left side of the peak at $2\theta = 3.50^\circ$, $q_z = 0.250$ Å^{-1}; (*c*) right side of the peak at $2\theta = 3.66^\circ$, $q_z = 0.260$ Å^{-1}. Dashed line: the experimental curve, solid line: the calculated one.

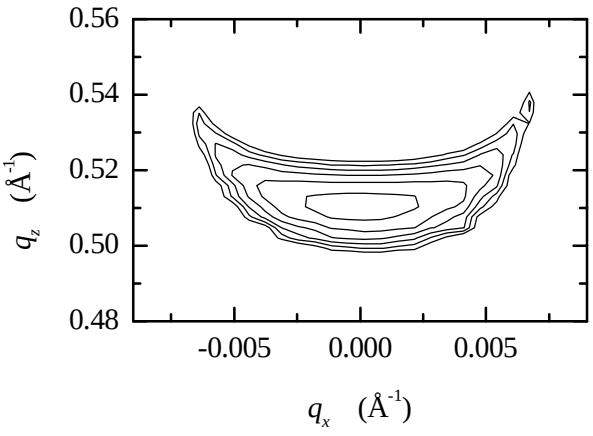

Figure 3. The diffuse scattering intensity distribution around the first Bragg peak in reciprocal space calculated using the DWBA method taking the x-ray refraction in the multilayer into account. The structural parameters of the [NiFe/Mo]$_{30}$ are: $t_{NiFe} = 17.0$ Å and $t_{Mo} = 8.2$ Å. The correlated roughness parameters are: $\xi = 100$ Å, $h = 1.0$ and $\sigma_{cor} = 3.6$. The neighbouring contours represent the intensity ratio $10^{0.4}$.

Similar experiments were also performed for samples N2 ($t_{NiFe} = 17.0$ Å and $t_{Mo} = 16.5$ Å) and N3 ($t_{NiFe} = 20.5$ Å, $t_{Mo} = 13.5$ Å). Figure 4(*a*) shows the small angle reflection (θ–2θ scan) curves of the samples N2 and N3. The rms of the total interfacial roughness of samples N2 and N3 was obtained by simulating the small angle reflection curves and was found to be $\sigma = 5.0 \pm 0.2$ Å and $\sigma = 3.0 \pm 0.2$ Å respectively (table 1). Figure 4(*b*) shows the transverse scans of samples N2 and N3. The rms of the correlated roughness of samples N2 and N3 was found to be $\sigma_{cor} = 3.9 \pm 0.2$ Å and 1.2 ± 0.2 Å respectively. Therefore, the rms of the uncorrelated interfacial roughness can be obtained: $\sigma_p = 3.1 \pm 0.4$ Å for sample N2 and $\sigma_p = 2.7 \pm 0.4$ Å for sample N3. The lateral correlation length of the correlated interfacial roughness was found to be $\xi = 300 \pm 50$ and 500 ± 50 Å respectively (table 2).

The origin of this uncorrelated component of the interfacial roughness has been evidenced in a previous high angle diffraction study on similar [NiFe/Mo]$_{30}$ multilayer samples [7]. In this study we revealed that there is a transition layer between the NiFe and Mo layers. The lattice parameter of this layer varied linearly from the bulk NiFe value to that of Mo over a thickness of approximately three atomic planes [7]. From table 2 one can see that the uncorrelated roughnesses σ_p of samples N1, N2 and N3 are all about 3 Å which is consistent with our previous results. There are two distinct morphologies that this transition layer can adopt. The observed linear dependence on the lattice parameter can be explained by a linear interdiffusion profile across the interface. This diffused layer would not result in diffuse scattered radiation from the multilayer [5, 11]. Another possibility is that the lattice mismatch causes small random fluctuations at the interface. The resulting uncorrelated roughness relaxes the lattice mismatch. The out of plane lattice parameter variation would also be linear in this case. In contrast to the previous model, such a transition layer would produce diffuse scatter. However, because of the low roughness values obtained it has not been possible to distinguish between these two models of the transition layer.

Similar work to that described above has also been carried out on the [Fe/Mo]$_{30}$ multilayers. Figure 5 shows the small angle reflection curves of [Fe/Mo]$_{30}$ multilayers, samples F1, F2 and

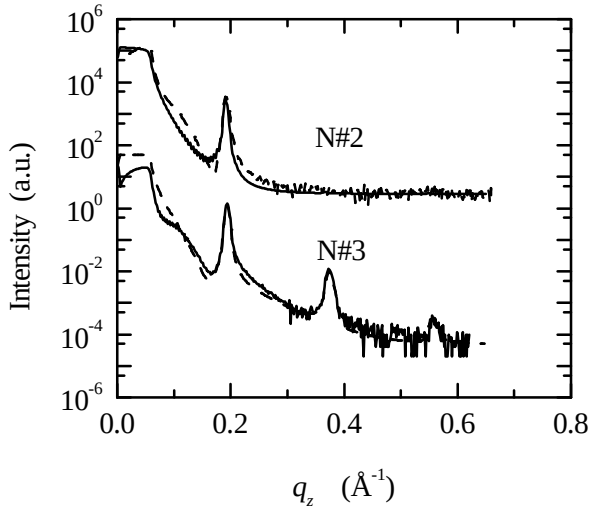

(*a*)

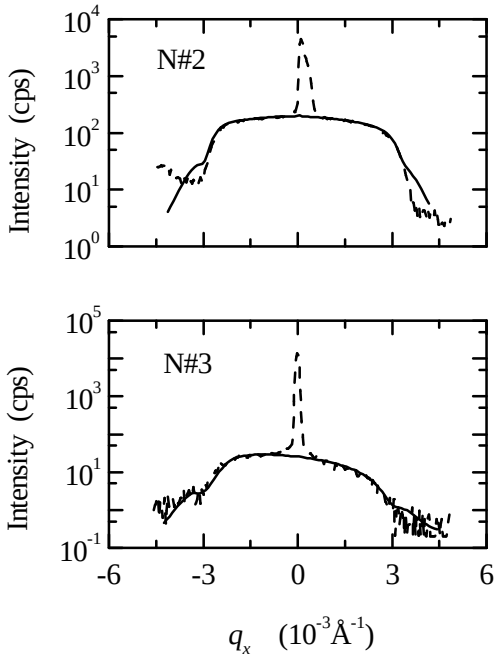

(*b*)

Figure 4. (*a*) Small angle reflection curves of samples N2 and N3: dashed line: the experimental curve, solid line: the simulated one. (*b*) The transverse scans of samples N2 and N3 with 2θ fixed at the first Bragg peak: dashed line: the experimental curve, solid line: the calculated one.

F3. In these samples the thickness of the Fe layer was fixed to 12 Å and the thickness of the Mo layer increased (table 3). Figure 6 shows the transverse scans through the Bragg peaks for the samples shown in figure 5. From figure 6, one can see that the specular peak

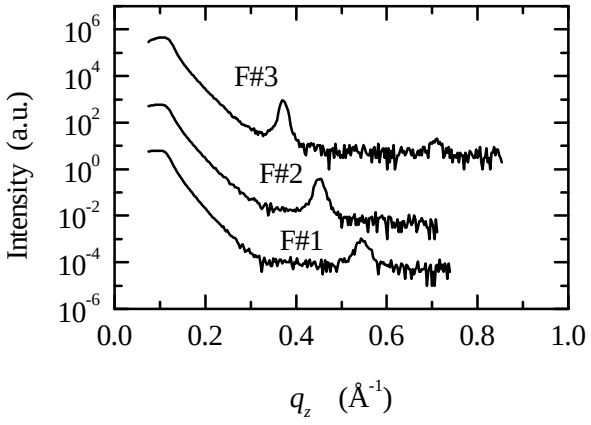

Figure 5. The small angle reflection curves of $[Fe/Mo]_{30}$ multilayers, F1, F2 and F3.

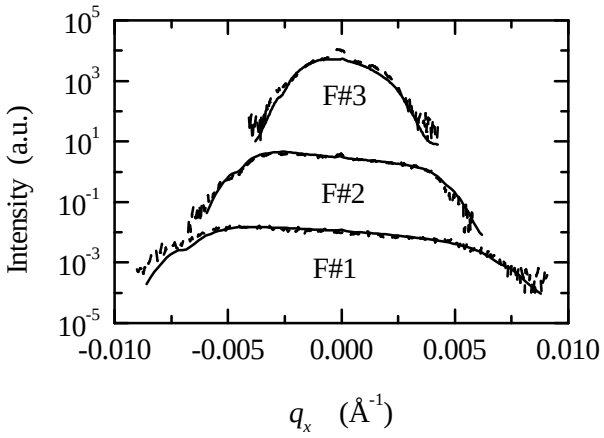

Figure 6. The transverse scans of $[Fe/Mo]_{30}$ multilayers, F1, F2 and F3 performed at the first Bragg peak. Dashed line: the experimental curve, solid line: the calculated one.

is very weak, and even disappears when the Mo layer thickness is 11.7 Å. Obviously the rms of the total interfacial roughness and the correlated interfacial roughness of the $[Fe/Mo]_{30}$ multilayers is larger than that of the $[NiFe/Mo]_{30}$ multilayers. Since the specular intensity in the transverse scans is very weak in the $[Fe/Mo]_{30}$ multilayers, it is difficult to obtain the rms of the total interfacial roughness and hence the correlated interfacial roughness. However, from the distribution of the diffuse scattering intensity in q_x, we can obtain lateral information on the correlated interfacial roughness by fitting the transverse scans. The lateral correlation lengths ξ of samples F1, F2 and F3 are 70 ± 10, 200 ± 50 and 800 ± 50 Å respectively, listed in table 3, and the exponents h of the $[Fe/Mo]_{30}$ multilayers are $0.5 \sim 0.6$, which is significantly different from that of $[NiFe/Mo]_{30}$ multilayers which were prepared by the same technique.

The shapes of the transverse diffuse scans shown in figure 6 are different from those obtained from the NiFe/Mo multilayers. In particular, there is an increase in the intensity at

Table 3. Interface parameters ξ and h of [Fe/Mo]$_{30}$ multilayers obtained from the transverse diffuse scatter.

Sample	t_{Fe} (Å)	t_{Mo} (Å)	ξ (Å)	h
F1	12	11.7	70 ± 10	0.5–0.6
F2	12	17	200 ± 50	0.5–0.6
F3	12	24	800 ± 50	0.5–0.6

high q_x in the Fe/Mo samples. This has been modelled by changing the fractal parameter for the Fe/Mo samples. A lower fractal parameter causes the diffuse intensity to be enhanced in high q_x regions because an x-ray scattering experiment does not yield $C_{ij}(R)$ directly, but its respective Fourier transform. In the [Fe/Mo]$_{30}$ multilayer, crystalline columns are observed by cross-section TEM [12]. Sharp fluctuations at the crystalline column edge induce a relatively large component of q_x in the Fourier spectrum, resulting in the observed lower fractal parameter. The value of ξ for [Fe/Mo]$_{30}$ samples increases with the increase of the Mo layer thickness, shown in table 3, indicating that the lateral size of the crystalline columns increases with the bi-layer period.

A comparison of the [NiFe/Mo]$_{30}$ multilayers with the [Fe/Mo]$_{30}$ shows that although their lattice mismatches are almost the same, about 8%, there are no crystalline columns in the [NiFe/Mo]$_{30}$ multilayers. The interface roughnesses of the [NiFe/Mo]$_{30}$ multilayers are also much smaller than those of the [Fe/Mo]$_{30}$ multilayers. Since there is a transition layer between the NiFe and Mo layers in [NiFe/Mo]$_{30}$ multilayers, the stress induced by the lattice mismatch is mainly relaxed at the interface. No such mechanism is possible in the [Fe/Mo]$_{30}$ multilayers. Here the Fe and Mo layers are matched inside the crystalline column, and the stress induced by the lattice mismatch is relaxed at the column edge. The different behaviour at the interface and the different growth mechanisms cause the interfacial roughness of the [NiFe/Mo]$_{30}$ samples to be much smaller than that of the [Fe/Mo]$_{30}$ multilayers.

The different interfacial states of the [NiFe/Mo]$_{30}$ and [Fe/Mo]$_{30}$ multilayers influence their magnetic properties. The relatively smooth interfaces of [NiFe/Mo]$_{30}$ induce large magnetic domains and pure interlayer coupling; furthermore typical alternating ferromagnetic and antiferromagnetic coupling hysteresis loops were observed as the Mo layer thickness changed [6]. The transition layer which has a high resistance between the NiFe and Mo sublayers also substantially reduces the mean free path of the electron, further depressing the magnetoresistance ratio of the [NiFe/Mo]$_{30}$ samples. This might be one of the reasons why no magnetoresistance could be observed in [NiFe/Mo]$_{30}$ multilayers, although typical ferromagnetic and antiferromagnetic hysteresis loops were observed [6].

In the [Fe/Mo]$_{30}$ multilayers, however, there exists a crystalline columnar structure with large interfacial roughness. When the Mo layer is 11.7 Å thick, the average lateral size of the crystalline columns is so small and the interface roughness so large that the multilayer becomes discontinuous. The fluctuated interface induces relatively large, static ferromagnetic coupling between the neighbouring Fe layers. As a result, besides the antiferromagnetic coupling between the neighbouring Fe layers, there is an obvious ferromagnetic coupling component which is also observed in the hysteresis loops when the Mo spacer layer is about 11 and 22 Å [6].

5. Summary

The interface states of [NiFe/Mo]$_{30}$ and [Fe/Mo]$_{30}$ multilayers were investigated by x-ray small angle reflection and diffuse scattering techniques. The rms of the geometrical roughness

of $[NiFe/Mo]_{30}$ multilayers is much smaller than that of $[Fe/Mo]_{30}$ multilayers. A transition layer of about 6 Å is observed in $[NiFe/Mo]_{30}$ multilayers, which is consistent with the results obtained previously from a high angle diffraction experiment. The fractal exponent h of about 0.5–0.6 was found for $[Fe/Mo]_{30}$ multilayers and its origin is attributed to the columnar growth of the multilayer. The results contained in this paper are helpful in understanding how the growth mechanisms affect the magnetic properties of $[NiFe/Mo]_{30}$ and $[Fe/Mo]_{30}$ multilayers.

Acknowledgments

The authors are grateful to Professor Z Zhang and Mr Y H Gao for their constructive discussions of the latest TEM results on $[NiFe/Mo]_{30}$ and $[Fe/Mo]_{30}$ multilayers. The work is supported by the Chinese Academy of Sciences under contract No KJ951-A1-401 and the National Natural Science Foundation of China.

References

[1] Parkin S S P 1994 Giant magnetoresistance and oscillatory interlayer coupling of polycrystalline transition metal multilayers *Ultrathin Magnetic Structure II* ed B Heinrich and J A C Bland (Berlin: Springer) pp 149–94
[2] Fullerton E E, Kelley D M, Guimpel J, Schuller I K and Bruynseraede Y 1992 *Phys. Rev. Lett.* **68** 859
Fullerton E E, Schuller I K, Vanderstraeten H and Bruynseraede Y 1992 *Phys. Rev.* B **45** 9292
[3] Nawate M, Inage K, Imada R, Itogawa M and Hodna S 1995 *Japan. J. Appl. Phys.* **34** 3082
[4] Savage D E, Kleiner J, Schimke N, Phang Y-H, Jankowski T, Jacobs J, Kariotis R and Lagally M G 1991 *J. Appl. Phys.* **69** 1411
[5] Li M, Mai Z H, Cui Q, Zhang L, Cui S F and Zhou J M 1994 *J. Appl. Phys.* **20**
[6] Yan M L, Lai W Y, Wang Y Z, Li S X and Yu C T 1995 *J. Appl. Phys.* **77** 1816
[7] Luo G M, Yan M L, Mai Z H and Lai W Y 1997 *Phys. Rev.* B **56** 3290
[8] Parratt L G 1954 *Phys. Rev.* **95** 359
[9] Sinha S K, Sirota E B, Garoff S and Stanley H B 1994 *Phys. Rev.* B **38** 2297
Sinha S K 1994 *J. Physique* III **4** 1543
[10] Holy V, Kubena J, Ohlidal I, Lischka K and Plotz W 1993 *Phys. Rev.* B **47** 15 896
Holy V and Baumbach T 1994 *Phys. Rev.* B **49** 10 668
[11] Schlomka J-P, Tolan M, Schwalowsky L, Seeck O H, Stettner J and Press W 1995 *Phys. Rev.* B **51** 2311
[12] Zhang Z, Gao Y H, Luo G M, Jiang H W and Lai W Y, An HREM Study of the Microstructure of Fe/Mo Magnetic Multilayers, to be submitted